https://doi.org/10.1016/j.jcsr.2017.12.011

A performance-based damage-control design procedure of hybrid steel MRFs with EDBs

Ke Ke[a,b,*], Michael CH Yam[b,c.]

[a]*College of Civil Engineering, Hunan University, Changsha, China*

[b]*Department of Building and Real Estate, The Hong Kong Polytechnic University, Hong Kong, China*

[c]*Chinese National Engineering Research Centre for Steel Connection, The Hong Kong Polytechnic University, Hong Kong, China*

Abstract:

A noteworthy feature of the hybrid steel moment resisting frames (MRFs) with energy dissipation bays (EDBs) is the damage-control behaviour characterised by concentration of plastic damages in the energy dissipation bay (EDB) under earthquakes. This paper presents a design methodology for conducting the damage-control design of hybrid steel MRFs with EDBs. First, the structural damage-control behaviour quantified by the classical bilinear kinematic hysteretic model with significant post-yielding stiffness ratio is clarified utilising the test results extracted from a large-scale quasi-static test programme. Then, based on the seismic energy balance of single-degree-of-freedom systems incorporating significant post-yielding stiffness ratios, the design philosophy and governing energy balance equations featuring the damage-control behaviour of low-to-medium rise hybrid steel MRFs with EDBs under earthquake ground motions are presented. Subsequently, a stepwise design procedure that can be used to search for a design strategy of a hybrid steel MRF with EDBs under expected ground motions is developed. Three low-to-medium rise prototype structures are designed by the proposed methodology, and the seismic responses of the systems are evaluated by pushover analyses and nonlinear response history analyses based on numerical models validated by the test results. The results indicate that all the prototype hybrid steel MRFs with EDBs can achieve the damage-control behaviour with the prescribed drift threshold, and hence the post-earthquake residual deformations are also mitigated. Since the proposed method is a direct-iterative design procedure, it also retains practical attractiveness and will ~~greatly~~ facilitate the seismic design of hybrid steel MRFs with EDBs.

Keywords: hybrid steel, energy dissipation bay, damage-control, energy balance

---

* Corresponding author.

Email address: keke@hnu.edu.cn

1. Introduction

Although ductility-based seismic design philosophy enables designers to develop seismic resistant structures with a ductile manner under expected earthquakes, it would result in excessive exploitation of plastic energy dissipation of structural members. Consequently, significant post-earthquake residual deformations may be developed and hence lead to long occupancy suspension for repairing works or even complete demolition of the structure, as shown by recent earthquake events and seismic loss estimations. For steel moment resisting frame (MRF) structures which are widely used in seismic regions ~~and have long been recognised as effective seismic resistant structures~~, recent research findings [1] indicate that a steel MRF designed according to the ASCE 7-05 standard would have a high potential of being a total economic loss even after a design-level earthquake ground motion due to unacceptable post-earthquake residual deformations. Driven by a growing appeal for resilient seismic engineering [2, 3] and more sustainable seismic resistant structures, the conventional design methodologies for steel MRFs may need to be reviewed, and the idea of enhancing the seismic performance of steel MRFs with preferable nonlinear behaviour and controllable post-earthquake residual deformation ~~after an earthquake event~~ is currently pursued by research communities.

In parallel with newly emerged innovative structures such as self-centring steel MRFs [4-7], a promising alternative for enhancing seismic performance of steel MRFs is to incorporate the damage-control behaviour [8-10] that restricts inelastic deformations to occur within expected structural components in a wide deformation range~~ to minimise post-earthquake repairing works~~. Therefore, damage-control steel MRFs with prescribed energy dissipation mechanisms that can be readily repaired~~, which also retain practical attractiveness,~~ are very much desirable. Apart from strategies that utilise supplementary energy dissipation devices [11-14] to realise the damage-control behaviour, a compact solution is to extend the dual-steel-based [15-17] or the hybrid-steel-based [18, 19] concept to steel MRFs. In particular, applying members of various steel grades in a steel MRF can lead to ideal damage evolution modes ~~and expected yielding sequences~~ under seismic actions, and thus facilitate plastic damage concentration in target members~~ to achieve the damage-control behaviour~~. For instance, Charney and Atlayan [18] developed the concept of hybrid steel MRF composed of steel frame members with various steel grades, and the satisfactory damage-control behaviour of the systems was validated by analyses of prototype structures. Tenchini *et al.* [16] initiated an investigation on the seismic response of dual-steel MRFs composed of high strength steel (HSS) and mild carbon steel members, and the satisfactory damage evolution mode of the prototype structures was also observed. Recently, Ke and Chen [8] proposed a hybrid steel MRF constructed by a HSS main frame and energy dissipation bays (EDBs) equipped with sacrificial energy dissipation beams. Under seismic actions, yielding of the sacrificial energy dissipation beams of mild carbon steel in the EDBs would be triggered before damage inception of the main frame, and the EDBs can ~~be the primary source of~~produce plastic energy dissipation in the "damage-control stage". When the system responds in this stage, the elastic HSS main frame can also provide significant recentring force, and thus lead to yielding of the EDBs during unloading and pull the structure back close to the original position [8]. Therefore, the post-earthquake residual deformation of a hybrid steel MRF with EDBs is also reduced compared with a conventional steel MRF. The sound seismic performance and encouraging failure mode of the hybrid steel MRF with EDBs have been demonstrated by a large-scale quasi-static experiment [8].

Owing to the yielding sequence of members in a hybrid steel MRF with EDBs under an earthquake event, the damage-control behaviour will restrict inelastic damages within pre-selected members in a wide deformation range. When the system deforms beyond the damage-control stage, inelastic actions of all members will contribute to plastic energy dissipation for balancing the demand of extreme seismic event. From the perspective of response curve of the hybrid steel MRF with EDBs under seismic actions, i.e. base shear versus lateral displacement response, multiple yielding stages [8, 20] of the hybrid steel MRFs with EDBs will result in hysteretic behaviour transformation, which is a critical issue in seismic design. Thus, explicit consideration of the damage-control stage of the system is a fundamental element for developing a full-fledged performance-based seismic design framework for the hybrid steel MRF with EDBs. However, the commonly used seismic design methodologies, which normally focus on the ultimate state of a structure concerning the life-safety objective, were mostly developed based on elastic-perfectly plastic (EPP) models, and hence may not be applicable for quantifying the damage-control behaviour of a hybrid steel MRF with EDBs described by the bilinear kinematic hysteretic model with significant post-yielding stiffness ratio [8]. In this context, even though it is in a preliminary design phase, performing a nonlinear response history analysis (NL-RHA) under expected ground motions may be required to obtain a design strategy, hence complicating the seismic design of a hybrid steel MRF with EDBs ~~greatly~~.

The present study is a continuation of the previous experimental programme [8] ~~towards a more in-depth understanding of the seismic resistance mechanism of the hybrid steel MRF with EDBs. The results of the study also~~ and contributes towards a practical design framework for quantifying the structural damage-control behaviour of the hybrid steel MRF with EDBs under expected earthquake ground motions. The proposed design method is based on the modified energy balance concept [21, 22]. First, based on the experimentally validated hysteretic model that quantifies the nonlinear behaviour of the hybrid steel MRF with EDBs in the damage-control stage, the fundamental principles of the methodology are clarified and the governing energy balance equations of low-to-medium rise hybrid steel MRFs with EDBs are deduced utilising the single-degree-of-freedom (SDOF) analogy. Subsequently, a stepwise damage-control design procedure of hybrid steel MRFs with EDBs, which is based on the concept of recently expanded performance-based plastic design (PBPD) methodology [23-30], is presented in detail. The proposed procedure is then applied to designing prototype structures of hybrid steel MRF with EDBs, and the effectiveness of the procedure for explicitly accounting for the damage-control behaviour of the novel system ~~hybrid steel MRF with EDBs~~ is justified by pushover evaluations and NL-RHA of numerical models of the designed systems under an ensemble of earthquake ground motions.

2. Seismic behaviour of hybrid steel MRFs with EDBs

The concept of the hybrid steel MRF with EDBs is shown in Fig. 1a. To trigger the early yielding behaviour of the EDBs, the sacrificial beams in the EDBs should be designed with relatively higher lateral stiffness but lower strength compared to the members in the main frame. At its core, applying the hybrid-steel-based concept in a steel MRF is a promising solution for decoupling the inherent interdependence between stiffness and strength of structural members, i.e., beams and columns in the structure, which generally initiate inelastic actions in rapid succession under earthquake events. A rational combination of the sacrificial energy dissipation beams in the EDBs and structural members with higher steel grades in the main frame can produce a damage-control stage in the pushover curve or skeleton response under seismic actions. ~~, leading to restriction of inelastic actions in the EDBs (Fig. 1b).~~ Thus, the cyclic response quantified by the classical bilinear kinematic model incorporating significant post-yielding stiffness ratio (Fig. 1b) can be extracted from the pushover curve or the skeleton response, which was ~~also~~ found to be effective for mitigating seismic residual deformation under earthquake events [31].

To provide test evidence for the proposed structural concept, a proof-of-concept study [8] has been recently accomplished utilising a large-scale quasi-static test programme of a hybrid steel MRF with EDB. In particular, the EDB with the sacrificial energy dissipation beams with reduced beam section (RBS) were combined with the HSS main frame. Core details of the test programme including the specimen and the test setup, are reproduced in Fig. 2a and Fig. 2b, respectively. The information about the beam members and column members is reproduced in Table 1 along with the actual material properties extracted from coupon tests. To clarify the damage-control behaviour, the storey shear of the second floor (V_2) of the specimen is plotted against the corresponding inter-storey drift (θ_2) and compared with the multi-linear idealisation [8] in different yielding stages, as shown in Fig. 2c. As can be seen in the figure, a desirable "damage-control core" described by the bilinear kinematic model with a significant post-yielding stiffness ratio can be extracted from the cyclic response~~ when the specimen responded in the damage-control stage~~. According to strain readings from strain gauges mounted on the specimen, the sacrificial energy dissipation beams in the EDB dissipated plastic energy stably and the main frame of HSS generally stayed elastic ~~in this stage~~when the specimen responded in the damage-control core. In addition, ~~It is worth pointing out that~~ the specimen also exhibited unexpectedly ~~excellent~~ ductile performance when it was loaded to significant deformations beyond the damage-control stage, and the failure mode of the specimen after the load cycle with the maximum inter-storey drift amplitude of 8% is also shown in Fig. 2d.~~ More details of the test programme can be found in [8]~~.

3. Design philosophy of the proposed procedure

3.1. Objectives and scopes

~~Responding to the demand of resilient seismic engineering and more sustainable seismic resistant systems, a design strategy of a hybrid steel MRF with EDBs achieving damage-control behaviour under expected earthquake ground motions is in urgent need. T~~The core of the present study is to develop a practical design procedure for low-to-medium rise hybrid steel MRFs with EDBs achieving damage-control behaviour under expected earthquake ground motions. The method follows the fundamental philosophy of the recently developed performance-based plastic design (PBPD) methodology [23-30] associated with the modified energy balance concept [21, 22]. Recognising that the hysteretic characteristics of the force-displacement response also ~~imposes an appreciable effect on~~ influence the seismic energy balance [20, 32] of a hybrid steel MRF with EDBs, an equivalent single-degree-of-freedom (SDOF) system with the bilinear kinematic hysteretic model incorporating significant post-yielding stiffness ratio is utilised ~~to characterise the damage-control behaviour~~ when developing the procedure ~~of the hybrid steel MRF with EDBs~~. Notwithstanding the desirable ductile performance as observed in the test, it should be noted that ductility of steel generally decreases with increasing of yield strength, and hence the inelastic deformation capacity of the main frame constructed by HSS is compromised. Therefore, in the current research, EDBs are designed as the primary source of plastic energy dissipation, whereas the main frame is designed to respond elastically under design-level earthquake attacks, and a rigorous capacity design criterion will be specified. Special care should be made when exploiting the inelastic energy dissipation of the main frame, which is not within the scope of this study. ~~In this context, the developed procedure is primarily employed to quantify the behaviour of a hybrid steel MRF with EDBs in the damage-control stage, while the performance of the system in the ultimate state where all members initiate inelastic deformations is not within the scope of this study.~~

3.2. *Underlying assumptions*

The underlying assumptions ~~, which could influence the accuracy of the proposed design procedure,~~ are clarified as follows: (1) a low-to-medium rise hybrid steel MRF with

EDBs can be reduced to an equivalent SDOF system with the mass of the entire structure and dynamic properties (e.g. period and damping) of the fundamental vibration mode [21-30]; (2) The seismic action of earthquake ground motions can be simplified with invariant lateral load distributions [24-27, 33, 34]; (3) In the design phase, the maximum displacement profile of the system follows a linear pattern, resulting in a uniform drift distribution [24-27]; (4) The nonlinear structural pushover curve or skeleton curve can be simplified with multi-linear idealisation [8]; (5) The inflexion points are located at the centre of the beams and columns for estimating the yield drifts [35-37]; (6) The system will eventually develop the global yielding mechanism without soft storey failure, and plastic hinges will be triggered at beam ends and column bases [24-27] and (7) The P-Δ effect induced by the gravity load will not impose an appreciable influence on the pushover response of a hybrid steel MRF with EDBs in the damage-control stage, and hence can be neglected in the design phase [24-27]. It is worth pointing out that these assumptions have been ~~successfully extended~~ applied to seismic design and evaluation procedures in various structures in the literature (The related references are indicated after the corresponding assumptions stated above), and the viability of applying them in the hybrid steel MRF with EDBs will be strengthened through validations in later sections.

3.3. Energy balance and the nominal plastic energy demand in the damage-control stage

Based on the first assumption stated in Section 3.2, the behaviour of a low-to-medium rise hybrid steel MRF with EDBs can be described by an equivalent SDOF system, and hence the seismic energy balance of the entire structure can also be quantified by ~~the energy balance~~ that of the equivalent SDOF system integrated with the dynamic properties of the fundamental vibration mode. In particular, the modified energy balance equation of an SDOF system [21] is reproduced and given as

$$E_{\mathrm{a}} = \gamma_{\mathrm{e}}(\frac{1}{2}MS_{\mathrm{v}}^{2}) = E_{\mathrm{e}} + E_{\mathrm{p}} \tag{1}$$

where E_{a}= nominal absorbed energy of the SDOF system quantified by the covered area of the pushover curve; γ_{e}= energy factor; M= mass of the SDOF system; E_{e}= elastic energy; E_{p}= nominal plastic energy and S_{v}= pseudo-velocity. To characterise the damage-control stage of a low-to-medium rise hybrid steel MRF with EDBs, a bilinear SDOF system incorporating significant post-yielding stiffness ratio (α) [20] can be used. The energy factor of the SDOF system, which prescribes the nominal seismic energy demand of the hybrid steel MRF with EDBs under seismic actions can be derived and related with the nonlinear quantities of the entire structure, as shown in Fig. 3a. This index is given as:

$$\gamma_{\mathrm{e}} = \frac{E_{\mathrm{a}}}{E_{\mathrm{ae}}} = [2\zeta - 1 + \alpha(\zeta - 1)^{2}]\chi \tag{2}$$

$$\chi = \frac{1}{R_{\mathrm{y}}^{2}} \tag{3}$$

$$R_{\mathrm{y}} = \frac{V_{\mathrm{e}}}{V_{\mathrm{ye}}} \tag{4}$$

where E_{ae}= absorbed energy of the corresponding elastic SDOF system featuring the behaviour of the hybrid steel MRF with EDBs responding elastically; ζ= ratio of the overall yield drift of the main frame to the overall yield drift of the EDBs; V_{ye} = base shear corresponding to inception of yielding of the EDBs; V_{e} = maximum base shear of the corresponding elastic hybrid steel MRF with EDBs; χ= damage-control factor~~. Although χ is dependent on the interactions among the hysteretic parameters (α and ζ), the dynamic properties of the system and the ground motion characteristics~~, and it can be generated directly using the recently developed algorithm for computing the energy factor of SDOF systems [20, 32]. To facilitate the design, based on the classical inelastic spectra proposed by Newmark and Hall [38], a set of design equations was also developed [39] for estimating χ, which are given as follows:

$$\chi = \begin{cases} \dfrac{1}{(2\dfrac{\zeta}{R_e}-1)R_e^2} & (\dfrac{T_1}{4} \le T < T_1^{'}) \\ \dfrac{1}{\dfrac{T^2}{T_1^2}\zeta^2} & (T_1^{'} \le T < T_1) \\ \dfrac{1}{\zeta^2} & (T_1 \le T) \end{cases} \tag{5}$$

$$R_e = \zeta - \sqrt{\zeta^2 - [\alpha(\zeta-1)^2 + 2(\zeta-1) + 1]} \tag{6}$$

where T_1= 0.57s and $T_1^{'} = T_1(\dfrac{\sqrt{2\dfrac{\zeta}{R_e}-1}}{\dfrac{\zeta}{R_e}})$. The detail of the derivation of the developed design equations can be found in [39].

~~Considering the assumption that a low-to-medium rise structure can be idealised by a SDOF system~~ Accepting the first assumption in Section 3.2, the absorbed nominal plastic energy (E_p) by the equivalent SDOF system in the damage-control stage is identical to the sum of nominal plastic energy dissipated by the EDBs. ~~In particular, according to the original definition of the seismic energy balance equation of a SDOF system [21], E_p is the plastic energy covered by the pushover (skeleton) response by deducing the elastic energy (E_e) from E_a when the system reaches the maximum deformation.~~ For a hybrid steel MRF with EDBs in the damage-control stage, as the main frame stay elastic and produce no plastic energy dissipation, E_p can be determined by deducing the elastic energy absorbed by the main frame and the elastic energy of EDBs in the elastic range, as schematically indicated in Fig. 3b. Therefore, the term of nominal plastic energy (E_p) which is expected to be dissipated by the sacrificial energy dissipation beams in the EDBs can be determined and given by

$$E_{\mathrm{p}} = \eta \frac{1}{2} \gamma_{\mathrm{e}} M S_{\mathrm{v}}^2 = \eta \frac{W g T^2}{8\pi^2} \gamma_{\mathrm{e}} S_a^2 \tag{7}$$

where S_a = pseudo-acceleration coefficient; W= the seismic weight of the entire structure and g= gravitational acceleration and η= the ratio of the nominal plastic energy (E_p) to the nominal absorbed energy (E_a) below the damage-control threshold (Fig. 3b), which can be determined as follows:

$$\eta = \frac{2(1-\alpha)(\zeta-1)}{\alpha(\zeta-1)^2 + 2(\zeta-1) + 1} \tag{8}$$

3.4. *Design of the EDBs and the main frame*

The lateral load distribution pattern developed by Chao *et al.* [34], which has been ~~successfully~~ extended to seismic design of various systems [23-30], is utilised in this study and reproduced as follows:

$$F_i = C_{vi} V_{\mathrm{b}} \tag{9}$$

$$C_{vi} = (\beta_i - \beta_{i+1}) \left[\frac{w_{\mathrm{N}} S_{\mathrm{N}}}{\sum_{j=1}^{\mathrm{N}} w_j S_j} \right]^{0.75T^{-0.2}} \tag{10}$$

$$\beta_i = \left[\frac{\sum_{j=i}^{N} w_j S_j}{w_{\mathrm{N}} S_{\mathrm{N}}} \right]^{0.75T^{-0.2}} \tag{11}$$

where the F_i= lateral force in the ith floor; C_{vi}= shear factor; β_i= distribution factor at ith floor; V_b= base shear force; w_N= the seismic weight at the top floor; w_i= the seismic weight at the ith floor; S_N= height of the top floor measured from the ground level and S_i= height of the ith floor measured from the ground level.

Assuming that the plastic moment capacity of the EDBs follows the lateral load distribution pattern, the demand plastic moment of the EDBs (the sum) in the ith floor of the structure can be determined based on the energy balance principle, and given by

$$\sum \overline{M_{\mathrm{pe},i}} = \beta_i \frac{\frac{WgT^2}{8\pi^2}\gamma_{\mathrm{e}} S_a^2}{\theta_{\mathrm{ye}} \sum_{i=1}^{\mathrm{N}} (\beta_i)} \bullet \frac{2(1-\alpha)}{\alpha(\zeta-1)^2 + 2(\zeta-1)+1} \tag{12}$$

where $\sum \overline{M_{\mathrm{pe},i}}$ = sum of the plastic moment demand of the sacrificial energy dissipation beams in the EDBs of the $i$the floor and θ_{ye}= overall yield drift of the EDBs. Thus, the overall yield drift of the main frame (θ_{yf}) is determined by $\zeta\theta_{\mathrm{ye}}$.

To facilitate the design process, the hysteretic parameters (α and ζ) of the SDOF system should be related to the member parameters, i.e. sectional properties, dimensions, and material properties. Thus, to associate the yield drift with the member parameters, the classical method developed by Gupta and Krawinkler [35], which has been utilised extensively [36, 37] is used to estimate the yield drift of the EDBs in the ith floor, and the equation is given by

$$\theta_{\mathrm{ye},i} = \left(\frac{M_{\mathrm{pe},i} l_{\mathrm{e},i}}{6EI_{\mathrm{e},i}} + \frac{M_{\mathrm{pe},i} h_i}{6EI_{\mathrm{c},i}}\right) \tag{13}$$

where $M_{\mathrm{pe},i}$= plastic moment capacity of the sacrificial energy dissipation beam of the EDB in the ith floor; $l_{\mathrm{e},\ i}$= distance between the columns centreline of the EDBs; $I_{\mathrm{e},i}$=moment of inertia of the beams in the EDBs; $I_{\mathrm{c},i}$= moment of inertia of the columns; h_i= height of the floor and E= elastic modulus of the material. Similarly, the yield drift of the main frame of the ith floor ($\theta_{\mathrm{yf},\,i}$) is determined by

$$\theta_{\mathrm{yf},\,i} = (\frac{M_{\mathrm{pb},i} l_{\mathrm{m},i}}{6EI_{\mathrm{b},i}} + \frac{M_{\mathrm{pb},i} h_i}{6EI_{\mathrm{c},i}}) \tag{14}$$

where $M_{\mathrm{pb},i}$= plastic moment capacity of the beam used in the main frame in the ith floor; $l_{\mathrm{m},i}$= distance between the columns centreline of the main frame and $I_{\mathrm{b},i}$= moment of inertia of the beams in the main frame. To reach an optimised design, the yield drift of the EDBs ($\theta_{\mathrm{ye},i}$) and that of the main frame ($\theta_{\mathrm{yf},i}$) for all floors should approach the corresponding overall drifts. Thus, in a multi-storey structure (N storeys in total), the overall yield drift of the EDBs (θ_{ye}) and the main frame (θ_{yf}) can be estimated considering average values for all floors, given as follows:

$$\theta_{\mathrm{ye}} = \frac{\sum_{i=1}^{\mathrm{N}} \theta_{\mathrm{ye},i}}{\mathrm{N}} \tag{15}$$

$$\theta_{\mathrm{yf}} = \zeta \theta_{\mathrm{ye}} = \frac{\sum_{i=1}^{\mathrm{N}} \theta_{\mathrm{yf},i}}{\mathrm{N}} \tag{16}$$

Based on the work-energy principle [22] that the work done by external forces (lateral load distribution) is stored as elastic energy in the system before the system yields, the corresponding base shear V_{ye} can be deduced from the following equation:

$$\frac{1}{2} V_{\mathrm{ye}} \sum_{i=1}^{\mathrm{N}} C_{vi} \delta_{\mathrm{ye},i} = \frac{1}{2} M (\frac{T}{2\pi} \bullet \frac{V_{\mathrm{ye}}}{M})^2 \tag{17}$$

where $\delta_{\mathrm{ye},i}$= the lateral displacement of the ith floor under the lateral load distribution when the base shear (V_{b}) determined by Equation (9)-(11) reaches V_{ye}. Therefore, accepting the third assumption in Section 3.2, the lateral displacement of floors can be related with storey drifts, and V_{ye} can be derived and given as follows:

$$V_{\mathrm{ye}} = \frac{4\pi^2 M \theta_{\mathrm{ye}} \sum_{i=1}^{\mathrm{N}} C_{vi} S_i}{T^2} \tag{18}$$

On the other hand, when the main frame initiates inelastic deformation and results in expected global mechanism, force equilibrium equation can be established by

$$\sum_{i=1}^{\mathrm{N}} F_{\mathrm{i}} S_{\mathrm{i}} = \sum M_{\mathrm{pc},1} + \sum_{i=1}^{\mathrm{N}} M_{\mathrm{pb},i} + \sum_{i=1}^{\mathrm{N}} M_{\mathrm{pe},i} \tag{19}$$

where $\sum M_{\mathrm{pc},1}$ = sum of plastic moment capacity of the column bases. Substituting Equation (19) into Equation (9)-(11), V_{yf} is determined by

$$V_{\mathrm{yf}} = \frac{\sum M_{\mathrm{pc},1} + \sum_{i=1}^{\mathrm{N}} M_{\mathrm{pb},i} + \sum_{i=1}^{\mathrm{N}} M_{\mathrm{pe},i}}{\sum_{i=1}^{\mathrm{N}} C_{vi} S_i} \tag{20}$$

Thus, the hysteretic parameter α can be expressed by

$$\alpha = \frac{V_{\mathrm{yf}} - V_{\mathrm{ye}}}{(\frac{\theta_{\mathrm{yf}}}{\theta_{\mathrm{ye}}} - 1) V_{\mathrm{ye}}} \tag{21}$$

For the hybrid steel MRF with EDBs, one of the noteworthy features is the satisfactory recentring ability of the system compared with a conventional steel MRF, as also observed in the previous experimental observations [8]. To further mitigate the post-earthquake residual deformation of the system due to the inelastic deformation of the EDBs, it is recommended that the following relationship of the hysteretic parameters should~~, which was validated by experimental results,~~ be satisfied:

$$\alpha(\zeta - 1) > 1 \tag{22}$$

In the perspective of structural parameters, the following equation can be obtained by substituting Equation (18), (20), and (21) into Equation (22).

$$\frac{(\sum M_{\mathrm{pc},1}+\sum_{i=1}^{N}M_{\mathrm{pb},i}+\sum_{i=1}^{N}M_{\mathrm{pe},i})T^2}{4\pi^2 M(\sum_{i=1}^{N}C_{vi}S_i)^2\theta_{\mathrm{ye}}}>2 \tag{23}$$

Note that Equation (23) essentially reflects the optimum relationship between the strength of EDBs and that of the main frame.

4. A stepwise design procedure

Based on the core philosophy addressed in Section 3, a stepwise procedure which enables a designer to develop a structural design strategy realising the damage-control stage under expected ground motions, is established and provided as follows:

Step 1: Based on the architectural strategy, determine the shape of the damage-control core by selecting the target value of the post-yielding stiffness ratio ($\overline{\alpha}$) and the ratio of the overall yield drift of the main frame to the overall yield drift of the EDBs ($\overline{\zeta}$). Then, prescribe the target overall yield drift of the EDBs ($\overline{\theta_{\mathrm{ye}}}$) and that of the main frame ($\overline{\theta_{\mathrm{yf}}}$), respectively. To achieve a more satisfactory residual drift response, the relationship given in Equation (22) should be satisfied ($\overline{\alpha}=\alpha, \overline{\zeta}=\zeta$). It is also worth pointing out that as a significant α is effective for mitigating post-earthquake residual deformations and producing more predictable seismic response, an initial value of 0.5 for α prescribing the lateral stiffness of the main frame relative to the entire structure in the elastic stage can be used to initiate the design iteration.

Step 2: Estimate the fundamental period of the system. At the beginning of the design, code-based design equations for estimating the fundamental period of a steel MRF will be applicable as a practical starting point, and then the Rayleigh approximation [23] may be used in iterative steps. In cases where elastic structural models are established~~ in an~~

~~iterative process~~, the fundamental period can be determined by a frequency analysis.

Step 3: Calculate the energy factor (γ_e). From a practical application point of view, γ_e can be estimated by Equation (5) and (6)~~ based on the classical Newmark and Hall inelastic spectra~~. In the subsequent iterations, γ_e can be determined by inelastic spectral analysis to enhance the accuracy for determining this core demand index. A validated algorithm [20, 32] ~~following the original definition of the energy factor determined by Equation (2)-(4)~~ can be used to generate this demand index according to the provided ground motions.

Step 4: Design the EDBs. In this step, the actual overall yield drift of EDBs (θ_{ye}) is estimated by Equation (13) and (15), and the plastic moment capacity of the sacrificial energy dissipation beams in the EDBs should meet the demand quantified by Equation (12). Amendment of member sections in the EDBs may be needed to ensure that the sacrificial energy dissipation beams of all stories have the yield drifts close to each other. It is noted that since the yield drift is also associated with column sections, the preliminary design of columns should be conducted in this step.

Step 5: Design the main frame. In particular, after preliminarily designing the main frame members, i.e. beams and columns, the yield drift of the main frame is determined by Equation (14) and (16). The overall yield drift of the main frame (θ_{yf}) and the counterparts in each floor ($\theta_{yf,i}$) should approach the prescribed target drift ($\overline{\theta_{yf}}$).

Step 6: Modify the structural arrangement to adjust the storey stiffness and strength to explicitly account for the inter-storey drift distribution. It should be noted that although the assumption of the uniform inter-storey drift distribution has been adopted to facilitate the design procedure~~ and is widely utilised in design methodologies~~, the actual inter-storey drifts will be also dependent on the actual structural arrangement. In the present study, the practical design indices proposed by Lu *et al.* [40] for predicting the seismic inter-storey drift distributions, namely the storey capacity factor and regularity index of frame structures, are applied to quantify the potential effect of structural arrangement on the seismic inter-storey drift distributions of hybrid steel MRF with EDBs. In particular, a regularity index was constructed in [40] and given as

$$\alpha_{\mathrm{sc}} = \frac{i_{\mathrm{sc,min}}}{i_{\mathrm{sc,ave}}} \tag{24}$$

where α_{sc}= regularity index; $i_{\mathrm{sc,min}}$ = the minimum storey capacity factor and $i_{\mathrm{sc,ave}}$= the average value of storey capacity factors considering all floors. In this study, a regularity vector is deduced from the indices in [40] and given as follows:

$$[\alpha_{\mathrm{sc}}] = [i_{\mathrm{sc},1}, i_{\mathrm{sc},2}, \ldots i_{\mathrm{sc,N}}] \tag{25}$$

To optimise the inter-storey drift distribution, the regularity vector should have uniformly distributed elements. The convergence criteria for this step is given by

$$\alpha_{\mathrm{sc}} \geq 0.9 \tag{26}$$

$$v = \mathrm{COV}[i_{\mathrm{sc},1}, i_{\mathrm{sc},2}, \ldots i_{\mathrm{sc,N}}] < 0.1 \tag{27}$$

where v = coefficient of variation of the storey capacity factors in the regularity vector. The detailed information about the definition of the storey capacity factor is provided in Appendix A.

Step 7: After obtaining a design strategy, go back to Step 1 to initiate the iterative process. In particular, the actual yield drifts quantities, i.e. θ_{ye} and θ_{yf} can be used to update $\overline{\theta_{\mathrm{ye}}}$ and $\overline{\theta_{\mathrm{yf}}}$. The hysteretic parameters α and ζ determined from Equation (15), (16), (18), (20) and (21) can be substituted into $\overline{\alpha}$ and $\overline{\zeta}$. Eventually, for a design strategy that can achieve the prescribed drift limit and realise the damage-control behaviour, the flowing criterion should be satisfied.

$$M_{\mathrm{pe},i} \geq \overline{M_{\mathrm{pe},i}} \tag{28}$$

In practice, designers can conduct a conservative design by properly increasing the plastic moment capacity of sacrificial energy dissipation beams in the EDBs.

Step 8: Check the section and other structural requirement of the structural members. To ensure that the assumption of global yielding mechanism holds, the column strength should be examined by a strong-column-weak-beam (SCWB) analysis, and the column tree method [34] which is used in the PBPD methodology will suffice. Also, Equation (23) should be satisfied to produce the controllable post-earthquake residual drifts.

A flow-chart of the stepwise procedure is illustrated in Fig. 4. ~~It is worth pointing out t~~ The fundamental logic of the procedure is in line with a direct-iterative design procedure, and ~~which is convenient for practical use and will enable a designer to develop design strategies based on expected earthquake ground motions.~~ it~~The iterative procedure~~ can be easily implemented in a standard spreadsheet programme. The demonstration of the proposed procedure will be presented in the later section.

5. Application of the design procedure

5.1. Ground motion ensemble

In the present study, an ensemble of twenty ground motion records (ground motions code LA01-LA20) [41] derived from historical records or from physical simulations is utilised as ground motions excitations, which was also adopted in the SAC projects and extensive research works for verification of the PBPD methodology [23, 25, 29]. These ground motion data can be viewed as design-based earthquake representatives for Los Angeles with a 10% probability of exceedance in 50 years, and the acceleration spectra corresponding to the damping ratio of 5% are given Fig. 5.

5.2. Implementation of the proposed design procedure

In the present work, three prototype hybrid steel MRFs with EDBs are designed according to the above proposed procedure. Two EDBs are used in the external bays for the 3-storey and the 6-storey structures, while three EDBs are considered for the 9-storey structure. The arrangement of the prototype structures are shown in Fig. 6. The dead load and the live load are assumed as 4.8 kN/m^2 and 2 kN/m^2. The seismic weight of the 3-storey, 6-storey and 9-storey hybrid steel MRFs with EDBs are 2509 kN, 5292 kN and 8771 kN, respectively. In the design procedure, the hysteretic parameters of α and ζ are selected, achieving the relationship in Equation (22). Then, the energy factor in the damage-control stage is initially estimated utilising the Equation (5) and (6). To produce the expected damage-control stage in the nonlinear pushover curve for the systems, the members in the prototype structures are designed with steel grades of Q235, Q390 and Q460 with the nominal yield strength of 235 MPa, 390 MPa and 460 MPa, respectively. The sacrificial energy dissipation beams in the EDBs is designed with the steel grade Q235, and reduced beam section (RBS) is incorporated to further compromise the strength of the beams for triggering the early yielding behaviour of the EDBs. The RBS sections are designed according to AISC 358 [42] and Chinese Code for Seismic Design of Buildings (GB 50011-2010) [43]. The plastic moment capacity of the centre of the RBS section are indicated in Fig. 6 by the values in brackets, and the detail of the RBS is provided in Appendix B. Note that the introduction of RBS detail in the EDBs would result in very slight reduction of the lateral stiffness of the system, and this effect is neglected in the case studies [8]. Recognising that the drift of 2% is currently adopted in the codified limit state for multi-storey steel MRFs [43], the threshold for damage-control stage is set below this limit. To explicitly account for the effect of structural stiffness and strength on the seismic inter-storey drift distributions, the regularity vector deduced from the indices proposed by Lu *et al.* [40] is adopted for adjusting the structural arrangement, and the critical indices are provided in Appendix C. The main parameters for the designed structures are provided in Table 2. For the purpose of demonstration, the iteration is considered once when applying the stepwise procedure, and the quantities obtained after the iteration are indicated by values in brackets in the table.

6. Validation of the design procedure

6.1. Verification of the energy factor

To validate the feasibility of Equations (5) and (6) for quantifying the energy factor of the hybrid steel MRFs with EDBs, the mean energy factor spectra of SDOF systems representing low-to-medium rise hybrid steel MRFs with EDBs are analysed by inelastic spectral analyses, covering a practical spectrum of α and ζ. The analysed mean energy factor spectra (damping ratio=5%) under the twenty ground motions stated in Section 5.1 are compared with the counterparts estimated by Equation (5) and (6) (solid lines), as shown in Fig. 7. For cases where α=0, Equation (5) and (6) reduce to the energy factor spectra deduced from the classical Newmark and Hall design spectra [21]. The good agreement between the results determined by Equation (5) and (6) and the energy factors extracted from inelastic spectral analyses is observed, although slightly unconservative estimates might be obtained for systems in the moderate-to-long period region with ζ increasing, which can be effectively eliminated by the spectral analyses in the iterative process as discussed in Section 4. ~~It can also be seen that both α and ζ impose an appreciable influence on the energy factor, echoing the rationality of the present study for considering the damage-control stage in seismic design frameworks.~~

6.2. Structural modelling and verification

The commercial software, Peform3D [44], is used to conduct a numerical study of the designed prototype structures. The modelling technique is first validated using the test results of the hybrid steel MRF with EDB from [8]. It is worth pointing out that the rationale of the modelling technique has been preliminarily validated in the previous work [8], whereas only the half of the twin frames and the idealised material nonlinearity, i.e. bilinear model with an assumed hardening ratio, were involved in the ~~previous analysis~~ model for simplification. To precisely account for the potential effect of the unsymmetric behaviour of the specimen, the twin frames in the specimen are modelled in the present study. For the EDB, the sacrificial energy dissipation beams are modelled with elastic frame segments and zero length plastic hinges, and the location of the plastic hinge coincides with the centre the RBS segments. For the main frame members, the inelastic fibre hinge method [8, 45, 46] is utilised, and a fibre segment length of 4% of the member length [45] is used. Shear deformation of panel zones is not considered for simplification. The braces between the twin frames are modelled by elastic truss elements. The general information about the model is shown in Fig. 8a. The trilinear kinematic hysteretic model is used to quantify the moment-rotation response of the beams and columns in the specimen, and the representative results are compared with the response curves of the members extracted from the test results, as given in Fig. 8b and Fig. 8c, respectively. The model does not employ fracture, local or global instability and cyclic degradation of members, and the simplification is rational in this study as the focus is given to the damage-control stage of the hybrid steel MRF with EDBs. To replicate the loading protocol in the test programme, the vertical loads (indicated in Fig. 8a) are applied on columns first using the measured data from the strain gauge readings, and ~~then~~ the cyclic loads on the two floors are applied subsequently. The comparisons of the response curves extracted from the test results and the counterparts from the numerical analysis, i.e. storey base shear versus inter-storey drift curve, are provided in Fig. 9. Since the fracture of structural members was observed at the inter-storey drift of 4% during loading process, the analysis is terminated in the corresponding cycle. In general, satisfactory agreement between the experimental data and the analysis results ~~extracted from the numerical model~~ can be observed.

6.3. Analysis results of the designed hybrid steel MRFs with EDBs

Based on the validated modelling technique, the designed prototype structures are simulated and both pushover evaluations and NL-RHA are performed to evaluate the seismic response of the systems. To examine the effectiveness of the discussion in Section 3.4 for quantifying the nonlinear behaviour of a hybrid steel MRF with EDBs in the damage-control stage, pushover analyses under the invariant lateral distribution determined by Equation (9)-(11) are carried out. To evaluate the P-Δ effect induced by gravity load on the nonlinear pushover curves of the system in the damage-control stage, two series of pushover analysis (P-Δ effect included and P-Δ excluded) are carried out for each prototype structure. The pushover responses in terms of base shear versus roof drift curves ~~of the three prototype structures~~ are provided in Fig. 10. The derived bilinear idealisation determined by Equation (15)-(21) are also identified in the figure. As can be seen, although the P-Δ effect would result in degradation of the post-yielding stiffness, the difference between the response curves determined from the pushover analysis including the P-Δ effect and the counterpart excluding the P-Δ effect is not evident in the damage-control stage before the main frames develop significant inelastic deformations. This observation is also in line with findings from previous studies, since the P-Δ effect is generally more evident in high rise structures designed to experience significant inelastic deformations [26], Also, good agreement between the pushover responses and the bilinear idealisation is observed, and the rationality of the proposed procedure is strengthened.

In the NL-RHA, the P-Δ effect is included, and a damping ratio of 5% is assumed for the first two vibration modes. The statistical results of the maximum inter-storey drift of the prototype structures in terms of mean, mean-plus-standard-deviation and mean-minus-standard-deviation are shown in Fig. 11. In general, relative uniform distribution of the maximum inter-storey drift is obtained, particularly in an average sense. The prescribed drift limit defined as the damage-control threshold is also indicated in the figure. As can be seen, the maximum inter-storey drift responses in average are below the prescribed limit drifts. These results indicate that the proposed design methodology is effective for performing a damage-control design by achieving the prescribed drift threshold with the provided ground motions.

Furthermore, the residual inter-storey drift responses of the designed structures under the input ground motions are shown in Fig. 12. The results under an individual ground motion and the mean responses under the twenty ground motions are all indicated. Note that to obtain the post-earthquake residual drift responses, the analysis time for NL-RHA is extended based on the ground motion duration, allowing for decaying of the structural vibration after an earthquake ground motion. In particular, the residual inter-storey drift for the 3-storey system in terms of mean value is 0.09%, while the counterparts for the 6-storey system and the 9-storey system are 0.04% and 0.09%, respectively. The residual inter-storey drift threshold of 0.5%, which can be perceivable by occupants and has been used to quantify the seismic resilience [1], is also indicated in the figure. Except for a very few cases in which the residual inter-storey drifts are above the threshold, i.e. the 3-storey structure under ground motion LA16 and the 6-storey structure under ground motion LA09 and LA11, all the systems exhibit quite satisfactory recentring behaviour with negligible residual inter-storey drifts. Note that when a hybrid steel MRF with EDBs achieve the damage-control behaviour under ground motions, all inelastic actions will be locked in the EDBs, and thus the residual deformations can be further mitigated by removing the damaged sacrificial energy dissipation beams in the EDBs.

6.4. Comments

It should be noted that as the primary objective of the present study is to develop a direct-iterative design procedure, certain degrees of trade-off between the theoretical rigorousness and the computational simplicity is made by introducing assumptions in the procedure, which have been utilised in other direct design procedures, e.g. the PBPD procedure [24-30]. However, from a practical application point of view, the procedure provides a promising tool to search for a preliminary strategy of a hybrid steel MRF with EDBs showing damage-control behaviour under expected ground motions, which is an essential component in a complete seismic design framework for extending the hybrid steel MRFs with EDBs in seismic regions. With the assistance of the proposed procedure, a designer can develop preliminary design strategies of hybrid steel MRF with EDBs efficiently. To finalise the design, modifications of the structural arrangement can be made with subsequent analysis works based on the design strategy produced by the proposed procedure, and potential inconsistent estimates of the seismic response induced by assumptions therefore can be effectively eliminated.

~~In summary, the paper puts forth a practical procedure for explicit consideration of the damage-control stage of hybrid steel MRF with EDBs. The proposed procedure allows a designer to obtain a preliminary design of the hybrid steel MRF with EDBs achieving the damage-control behaviour under provided earthquake ground motions, which is of great importance in performance-based seismic design.~~

7. Conclusions

As a promising seismic resistant system, the hybrid steel MRFs with EDBs were demonstrated to have sound seismic performance and encouraging damage evolution mode. By combining the EDBs equipped with sacrificial energy dissipation beams of mild carbon steel and the main frame of HSS, the damage-control behaviour of the system with restriction of plastic damages in the EDBs will be realised naturally in a wide deformation range, and a damage-control stage can be extracted from the pushover response curve under seismic actions. To rationally design a hybrid steel MRF with EDBs considering the damage-control stage, a design procedure of low-to-medium rise hybrid steel MRFs with EDBs is developed in this research. Following the basic philosophy of the PBPD procedure, the proposed method is a typical direct-iterative design approach, and the seismic demand is quantified by the energy factor deducing from the SDOF system with the hysteretic model validated by the test results. After relating the structural member parameters with the hysteretic parameters of the equivalent SDOF systems, a straightforward stepwise design procedure with computational attractiveness is established. The proposed procedure is applied to three low-to-medium rise prototype structures, and the robustness of the procedure is examined by nonlinear pushover evaluations and NL-RHA.

In general, the energy factor of SDOF systems with significant post-yielding stiffness ratios serves as a reliable index for quantifying the seismic demand of low-to-medium rise hybrid steel MRF with EDBs in the damage-control stage. The comparison of energy factors of SDOF systems incorporating various post-yielding stiffness ratios with the counterparts determined by the modified classical Newmark and Hall spectra strengthens the great potential of the developed practical equations for quantifying this core demand index reasonably. Moreover, as features of strength and deformation are employed in the energy factor, there will be no need to prescribe the limits for both strength and ductility, as adopted in conventional design methodologies, i.e. force-based or displacement-based design procedures.

The results extracted from the NL-RHA of the prototype structures indicate that the developed stepwise procedure is effective for achieving the maximum inter-storey drifts close to the damage-control threshold defined by a pre-selected target drift. The distributions of the maximum inter-storey drift in terms of the mean values are generally uniform along the structural height. Also, neglecting the P-Δ effect for computational simplicity in the stepwise procedure does not evidently compromise the accuracy for predicting the nonlinear pushover response curve in the damage-control stage, echoed by the good agreement between the results determined by pushover evaluations and the predicted nonlinear pushover curves by the proposed method.

It is worth pointing out that although the hybrid steel MRFs with EDBs realised by hybrid steel concept might increase the initial construction cost compared with that of a conventional steel MRF, the desirable damage evolution mode and the controllable residual inter-storey drift distributions of the prototype structures have demonstrated the great potential of the system for mitigating post-earthquake damages and minimising repair works, making the system both sustainable and economically viable in seismic regions.

Acknowledgments

This research is supported by the Fundamental Research Funds for the Central Universities of China (No. 531107050968). Partial funding supports provided by the Chinese National Engineering Research Centre for Steel Connection, The Hong Kong Polytechnic University (Project No. 1-BBYQ) and the National Natural Science

Foundation of China (Grant No. 51708197 and No. 51578228) are also gratefully acknowledged. The first author would like to thank Prof. Yiyi Chen at Tongji University, China for his constructive comments.

References

[1] Erochko J, Christopoulos C, Tremblay R, Choi H. Residual drift response of SMRFs and BRB frames in steel buildings designed according to ASCE 7-05. J Struct Eng. 2010; 137(5): 589-599.

[2] Bruneau M, Chang SE, Eguchi RT, et al. A framework to quantitatively assess and enhance the seismic resilience of communities. Earthq spectra. 2003; 19(4): 733-752.

[3] Cimellaro GP, Bruneau M. RAM. Framework for analytical qualification of disaster resilience. Eng Struct. 2010; 32(11): 3639-3649.

[4] Kim HJ, Christopoulos C. Seismic design procedure and seismic response of post-tensioned self-centering steel frames. Earthq Eng Struct Dyn. 2009; 38(3): 355-376.

[5] Iyama J, Seo CY, Ricles J, Sause R. Self-centering MRFs with bottom flange friction devices under earthquake loading. J Constr Steel Res. 2009; 65(2): 314-325.

[6] Lin Y, Sause R, Ricles J. Seismic performance of steel self-centring, moment-resisting frame: hybrid simulations under design basis earthquake. J Struct Eng. 2013; 4(11): 1823-1832.

[7] Fang C, Wang W, He C, Chen Y. Self-centring behaviour of steel and steel-concrete composite connections equipped with NiTi SMA bolts. Eng Struct. 2017; 150: 390-408.

[8] Ke K, Chen Y. Seismic performance of MRFs with high strength steel main frames

and EDBs. J Constr Steel Res. 2016; 126: 214-228.

[9] Ozaki F, Kawai Y, Kanno R, Hanya K. Damage-control systems using replaceable energy-dissipating steel fuses for cold-formed steel structures: seismic behaviour by shake table tests. J Struct Eng. 2012; 139(5):787-95.

[10] Connor JJ, Wada A, Iwata M, Huang Y. Damage-controlled structures. I: Preliminary design methodology for seismically active regions. J Struct Eng. 1997; 123(4): 423-431.

[11] Vargas R, Bruneau M. Experimental response of buildings designed with metallic structural fuses. II. J Struct Eng. 2009; 135(4): 394-403.

[12] Guo JWW, Christopoulos C. Performance spectra based method for the seismic design of structures equipped with passive supplemental damping systems. Earthq Eng Struct Dyn. 2013; 42(6): 935-952.

[13] Xu LY, Nie X, Fan JS. Cyclic behaviour of low-yield-point steel shear panel dampers. Eng Struct. 2016; 126: 391-404.

[14] He L, Togo T, Hayashi K, Kurata M, Nakashima M. Cyclic behaviour of multirow slit shear walls made from low-yield-point steel. J Struct Eng. 2016; 142(11): 4016094.

[15] Dubina D, Stratan A, Dinu F. Dual high-strength steel eccentrically braced frames with removable links. Earthq Eng Struct Dyn. 2008; 37(15): 1703-1720.

[16] Tenchini A, D'Aniello M, Rebelo C, Landolfo R, Da Silva LS, Lima L. Seismic performance of dual-steel moment resisting frames. J Constr Steel Res. 2014; 101: 437-454.

[17] Tenchini A, D'Aniello M, Rebelo C, Landolfo R, da Silva LS, Lima L. High strength

steel in chevron concentrically braced frames designed according to Eurocode 8. Eng Struct. 2016; 124: 167-185.

[18] Charney FA, Atlayan O. Hybrid moment-resisting steel frames. Eng J AISC. 2011; 48(3): 169-182.

[19] Atlayan O, Charney FA. Hybrid buckling-restrained braced frames. J Constr Steel Res. 2014; 96: 95-105.

[20] Ke K, Ke S, Chuan G. The energy factor of systems considering multiple yielding stages during ground motions. Soil Dyn Earthq Eng. 2015; 71: 42-48.

[21] Leelataviwat S, Saewon W, Goel SC. Application of energy balance concept in seismic evaluation of structures. J Struct Eng. 2009; 135(2): 113-121.

[22] Leelataviwat S, Goel SC, Stojadinović B. Energy-based seismic design of structures using yield mechanism and target drift. J Struct Eng. 2002; 128(8): 1046-1054.

[23] Pekcan G, Linke C, Itani A. Damage avoidance design of special truss moment frames with energy dissipating devices. J Constr Steel Res. 2009; 65(6): 1374-1384.

[24] Goel SC, Liao WC, Bayat MR, Chao SH. Performance-based plastic design (PBPD) method for earthquake-resistant structures: an overview. Struct Des Tall Spec Build. 2010; 19(1-2): 115-137.

[25] Sahoo DR, Chao SH. Performance-based plastic design method for buckling-restrained braced frames. Eng Struct. 2010; 32(9): 2950-2958.

[26] Kharmale SB, Ghosh S. Performance-based plastic design of steel plate shear walls. J Constr Steel Res. 2013; 90: 85-97.

[27] Yang TY, Li Y, Leelataviwat S. Performance-based design and optimization of

buckling restrained knee braced truss moment frame. Eng Struct. 2013; 60: 1-11.

[28] Wongpakdee N, Leelataviwat S, Goel SC, Liao WC. Performance-based design and collapse evaluation of buckling restrained knee braced truss moment frames. Eng Struct. 2014; 60: 23-31.

[29] Pekcan G, Itani AM, Linke C. Enhancing seismic resilience using truss girder frame systems with supplemental devices. J Constr Steel Res. 2014; 94: 23-32.

[30] Heidari A, Gharehbaghi S. Seismic performance improvement of special truss moment frames using damage and energy concepts. Earthq Eng Struct Dyn. 2015; 44(7): 1055-1073.

[31] Pettinga D, Christopoulos C, Parnpanin S, Priestley N. Effectiveness of simple approaches in mitigating residual deformations in buildings. Earthq Eng Struct Dyn. 2007; 36(12): 1763-1783.

[32] Ke K, Chuan G, Ke S. Seismic energy factor of self-centering systems subjected to near-fault earthquake ground motions. Soil Dyn Earthq Eng. 2016; 84: 169-173.

[33] Chopra AK, Goel RK. A modal pushover analysis procedure for estimating seismic demands for buildings. Earthq Eng Struct Dyn. 2002; 31(3): 561-582.

[34] Chao SH, Goel SC, Lee SS. A seismic design lateral force distribution based on inelastic state of structures. Earthq Spectra. 2007; 23(3): 547-569.

[35] Gupta A, Krawinkler H. Relating the seismic drift demands of SMRFs to element deformation demands. Eng J AISC. 2002; 39(2): 100-108.

[36] Chopra AK, Goel RK, Chintanapakdee C. Evaluation of a Modified MPA procedure assuming higher modes as elastic to estimate seismic demands. Earthq Spectra. 2004;

20(3): 757-778.

[37] Choi IR, Park HG. Steel Plate Shear Walls with Various Infill Plate Designs. J Struct Eng. 2009; 135(7): 785-796.

[38] Newmark NM, Hall WJ. Earthquake Spectra and Design. Earthquake Engineering Research Institute: Berkeley, CA, 1982.

[39] Ke K, Yam MCH. Energy-factor-based damage-control evaluation of steel MRF systems with fuses. Steel Compos Struct. 2016; 22(3): 589-611.

[40] Lu Y, Gu X, Wei J. Prediction of seismic drifts in multi-storey frames with a new storey capacity factor. Eng Struct. 2009; 31(2): 345-357.

[41] Shome N, Cornell CA, Bazzurro P, Carballo JE. Earthquakes, records, and nonlinear responses. Earthq Spectra. 1998; 14(3): 469-500.

[42] AISC. Prequalified connections for special and intermediate steel moment frames for seismic applications, ANSI/AISC 358-10. American Institute for Steel Construction: Chicago, IL, 2010.

[43] CMC. Code for seismic design of buildings (GB 50011-2010). China Ministry of Construction: Beijing, 2010

[44] CSI. PERFORM-3D v4.0.3 nonlinear analysis and performance assessment for 3D structures. California, USA: Computers and Structures Inc.; 2006.

[45] Cuong NH, Kim SE. Practical advanced analysis of space steel frames using fibre hinge method. Thin-Walled Struct. 2009; 47(4): 421-430.

[46] Thai HT, Kim SE. Second-order inelastic dynamic analysis of steel frames using fibre hinge method. J Constr Steel Res. 2011; 67(10): 1485-1494.

Appendix A

The core concept of the capacity factor proposed by Lu *et al.* [40] is to develop a practical method to relate the roof drift and the maximum inter-storey drift utilising curve fitting approach. In particular, the storey capacity factor is determined by

$$i_{sc} = i_{ns} \cdot i_{os} \tag{A.1}$$

where i_{ns} and i_{os} are the stiffness factor and the strength factor, respectively. For the stiffness factor in the *i*th floor, it can be estimated by

$$i_{ns} = (\frac{D}{V_s})_i \tag{A.2}$$

where D and V_s are the storey stiffness and the storey shear force demand. For practical applications, the storey stiffness is determined by the widely used D value-method. For the strength factor i_{os}, it is expressed as follows:

$$i_{os} = (\frac{V_R}{V_s})_i \tag{A.3}$$

where V_R is storey shear strength capacity. Since the global yielding mechanism is assumed and guaranteed in the proposed design procedure, V_R should be calculated based on the assumption that plastic hinges are triggered at beam ends. Also note that V_s follows the lateral load distribution utilised in this study.

It is noted that according to the observations from a previous research study [40], a value of α_{sc} approaching unity is a necessary prerequisite for a system realising the uniform inter-storey drift distribution.

Appendix B

The RBS details of sacrificial energy dissipation beams in the prototype structures are designed following GB 50011-2010 and AISC 358, and are given in Fig. B.1.

Appendix C

The storey capacity factors and regularity indices of the prototype structures are given in Table C.1-Table C.3.

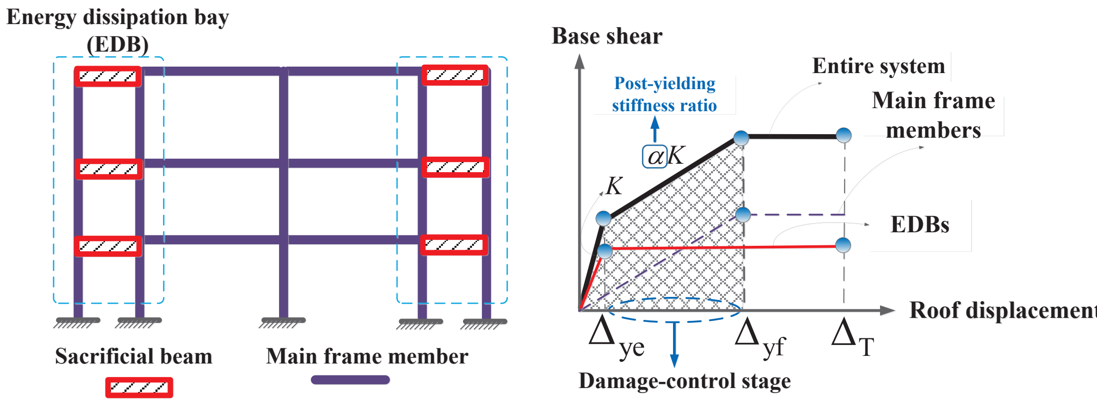

(a) (b)

Fig. 1 Structural concept of the hybrid steel MRF with EDBs [8]: (a) typical structural arrangement, and (b) idealised pushover (skeleton) response.

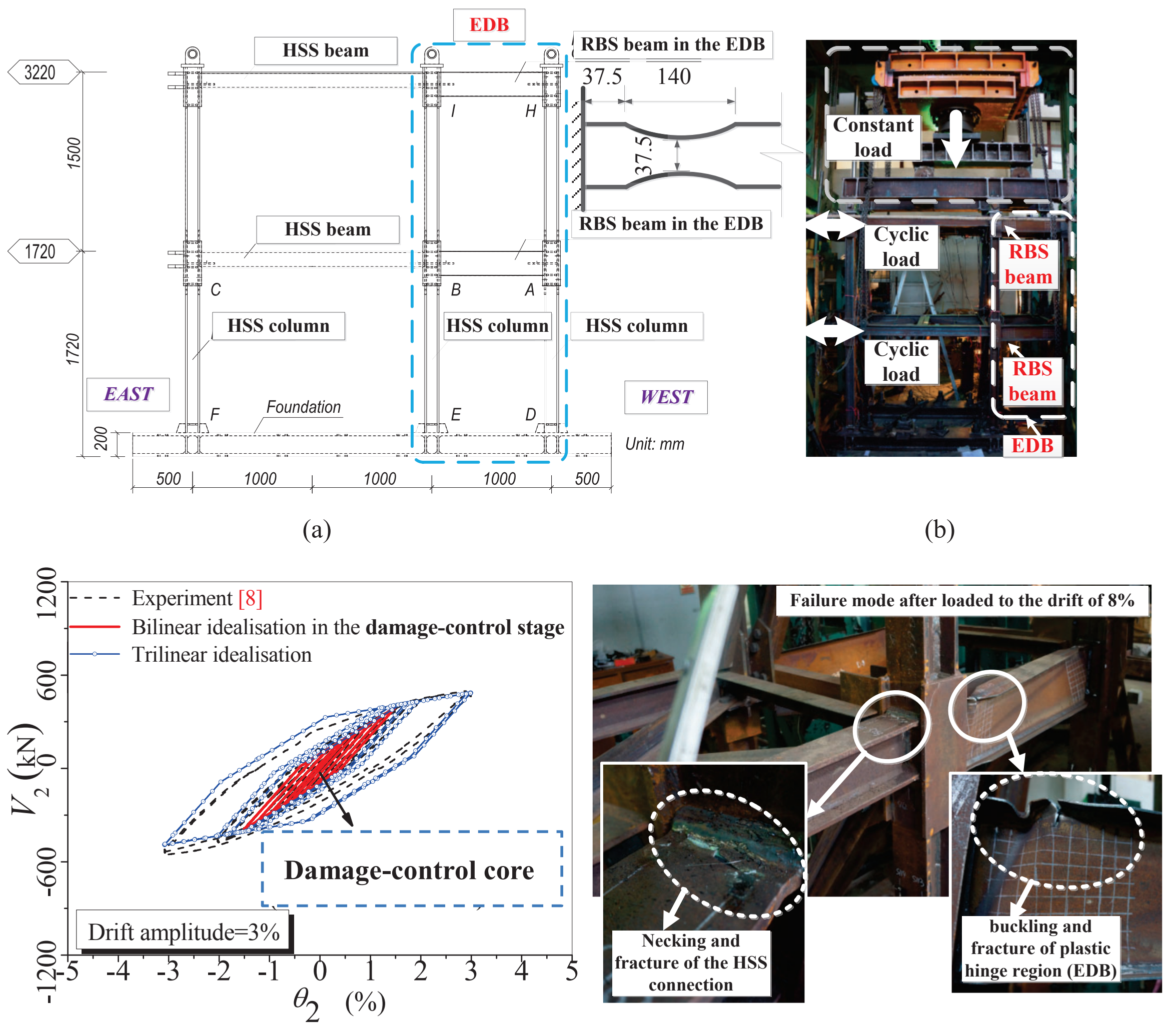

(c) (d)

Fig. 2 Test programme of a hybrid steel MRF with EDB [8]: (a) test specimen, (b) test setup, (c) cyclic response and (d) failure mode.

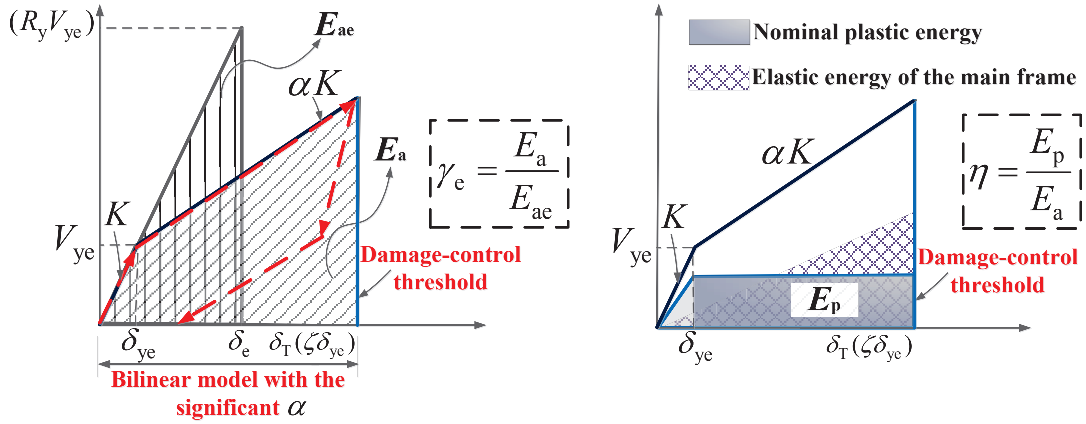

(a) (b)

Fig. 3 Energy balance of the equivalent SDOF system with significant post-yielding stiffness ratio: (a) energy factor [20], and (b) ratio of the nominal plastic energy to the nominal absorbed energy.

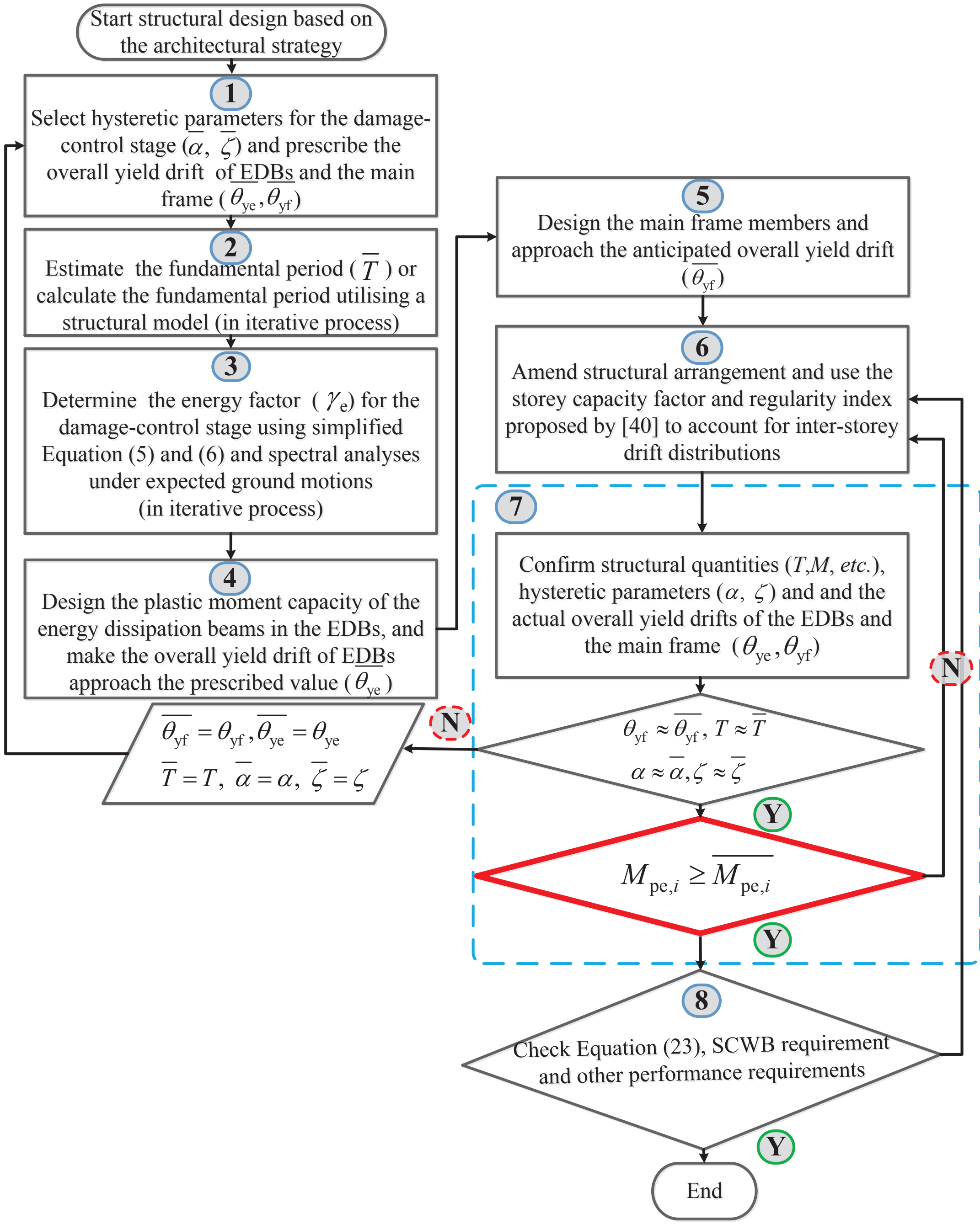

Fig. 4 Flow-chart of the proposed procedure.

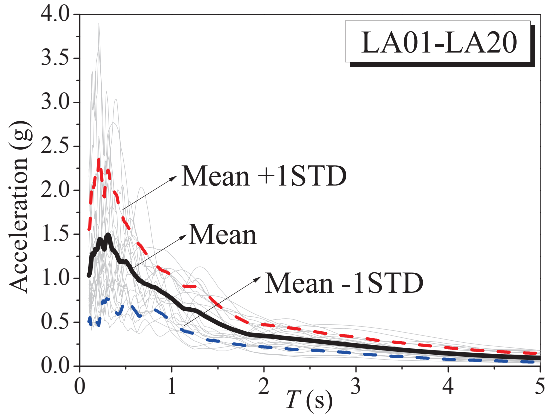

Fig. 5 Acceleration spectra of ground motions [41].

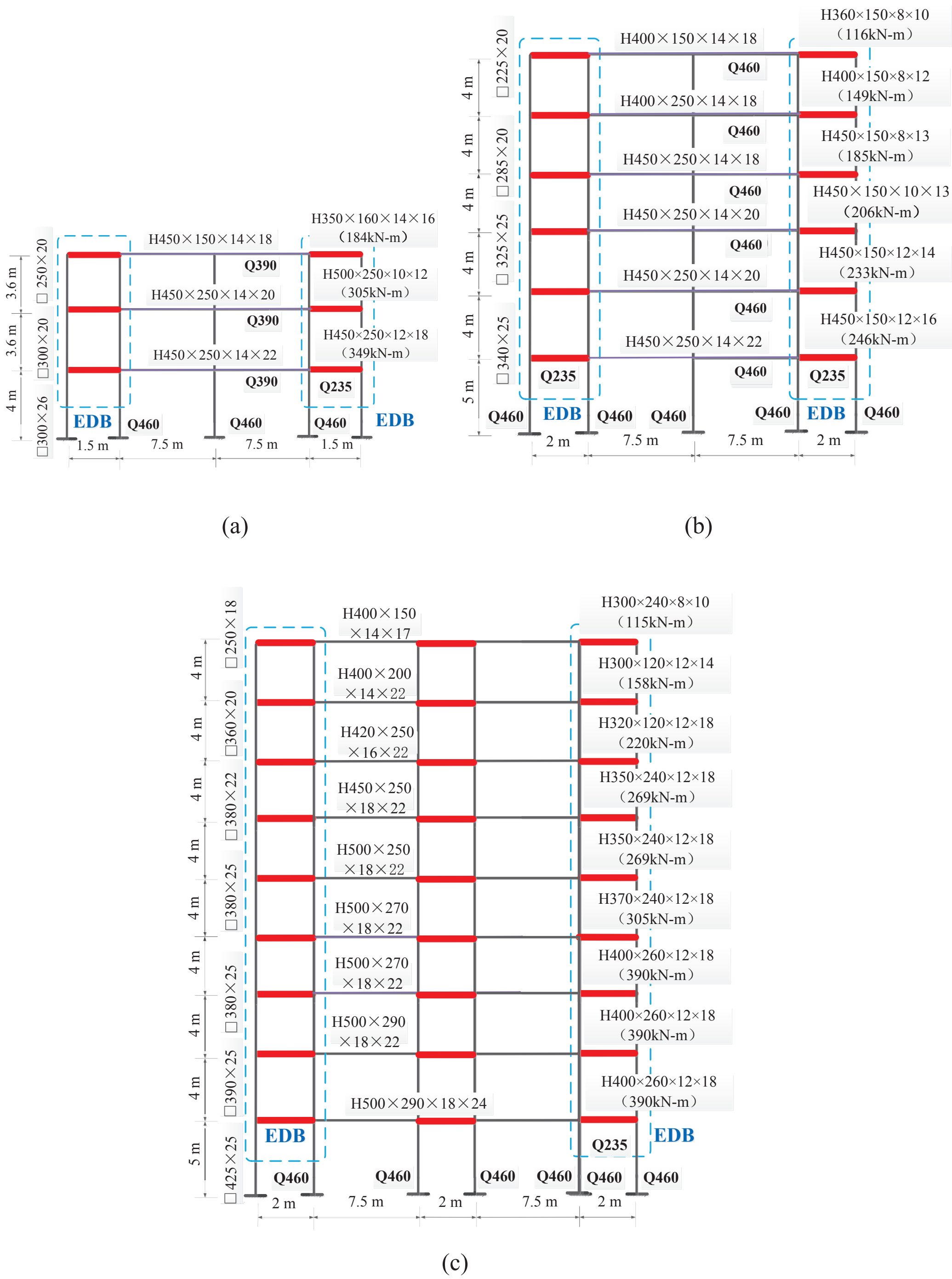

Fig. 6 Structural arrangement: (a) 3-storey structure, (b) 6-storey structure and (c) 9-storey structure.

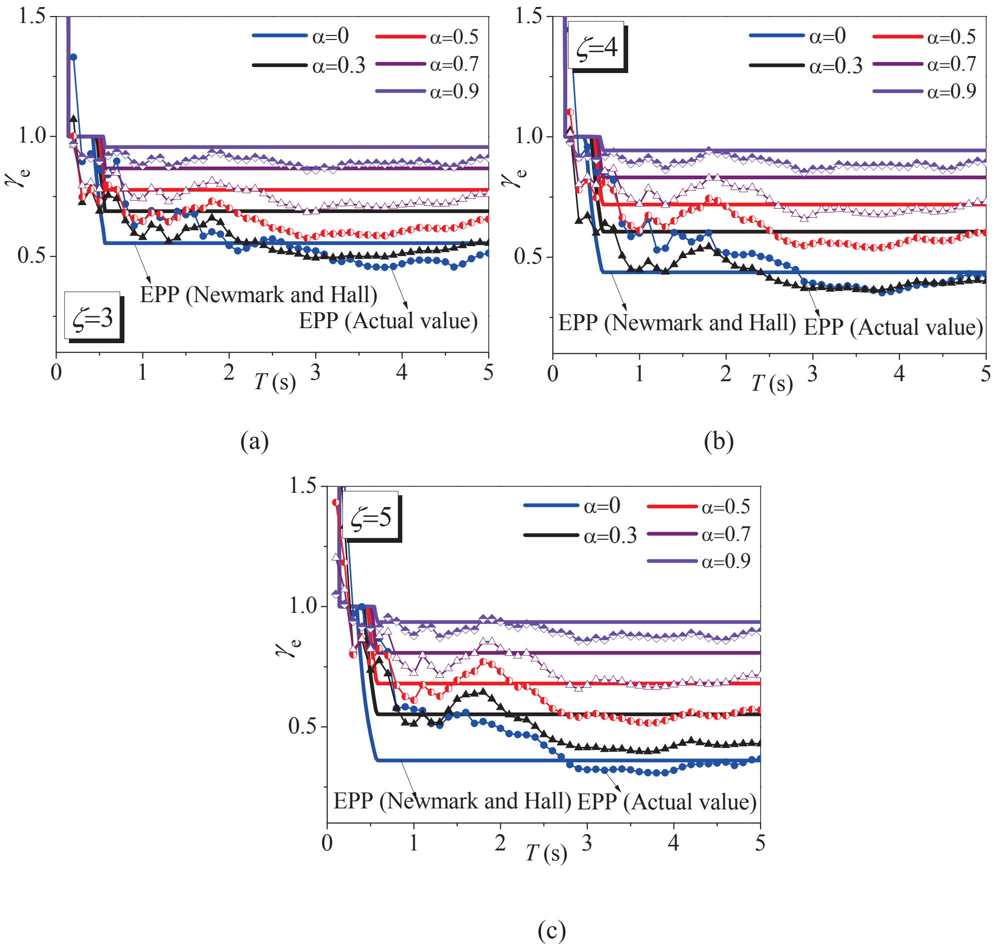

Fig. 7 Comparison of the energy factor spectra determined by the simplified equations [39] and counterparts from inelastic spectral analyses: (a) ζ=3, (b) ζ=4 and (c) ζ=5.

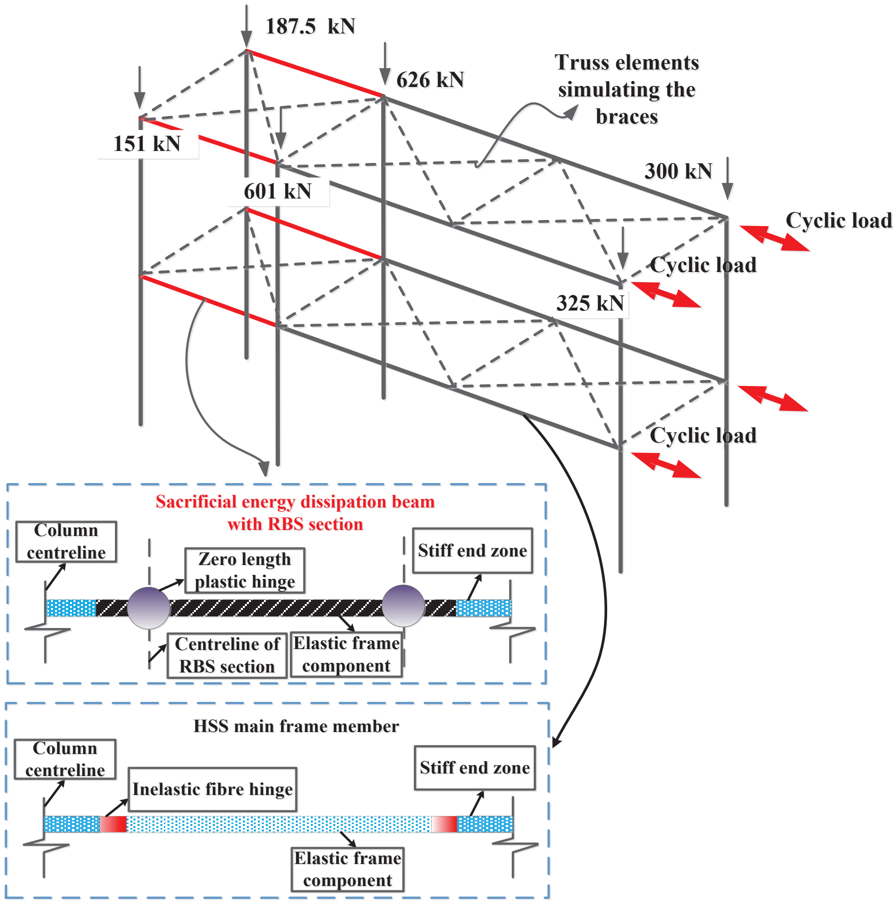

(a)

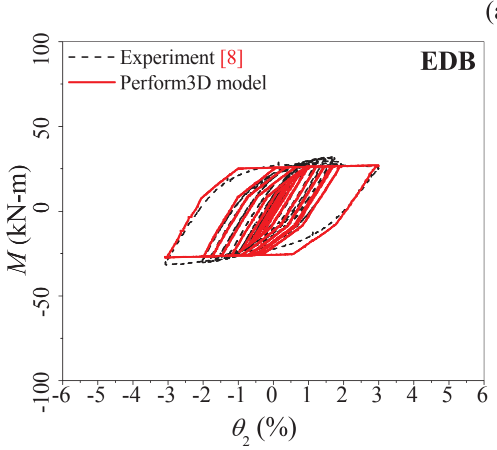

(b)

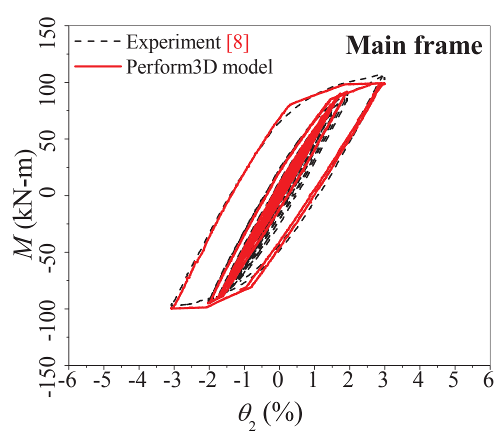

(c)

Fig. 8 Numerical models: (a) Modelling of the test specimen [8], (b) comparison of response curves of the representative sacrificial beam and (c) comparison of response curves of the representative HSS member.

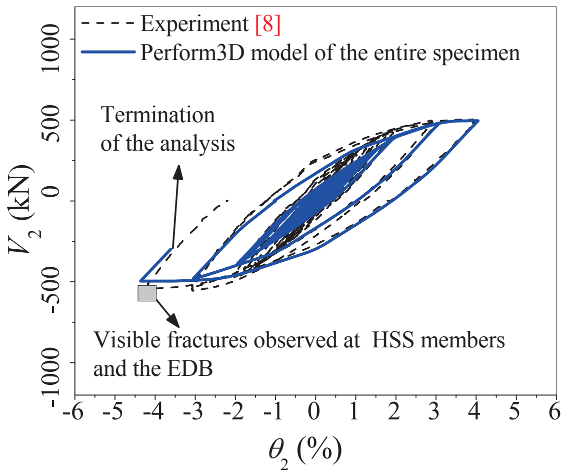

Fig. 9 Comparison of the hysteretic response extracted from the test data and analysis results.

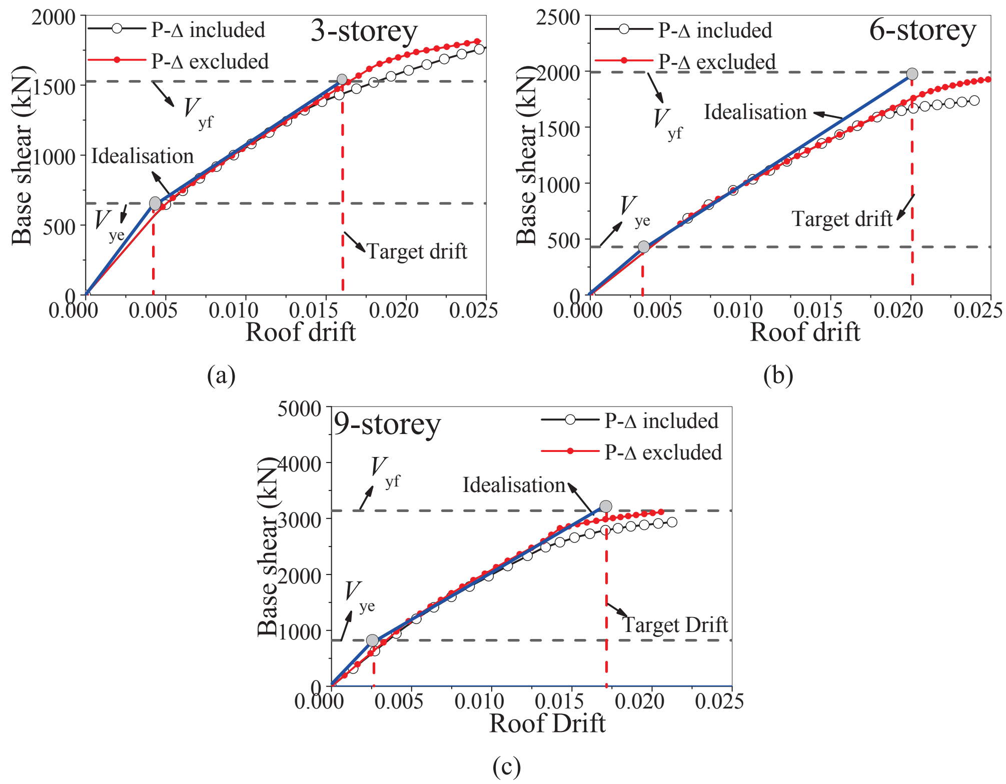

Fig. 10 Comparison of the pushover responses and the bilinear idealisations in the design procedure: (a) 3-storey structure, (b) 6-storey structure and (c) 9-storey structure.

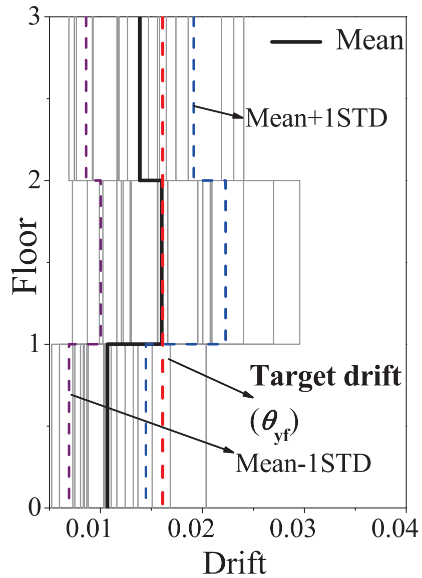

(a)

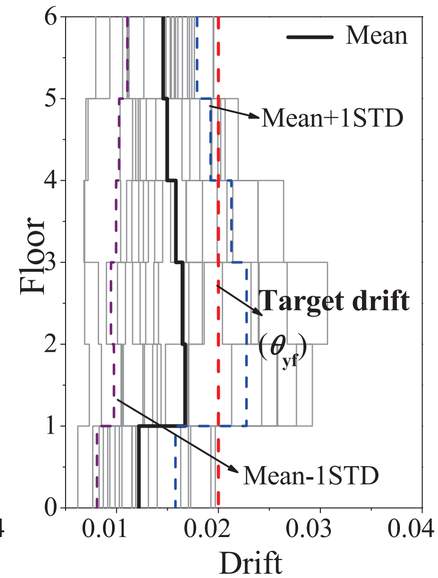

(b)

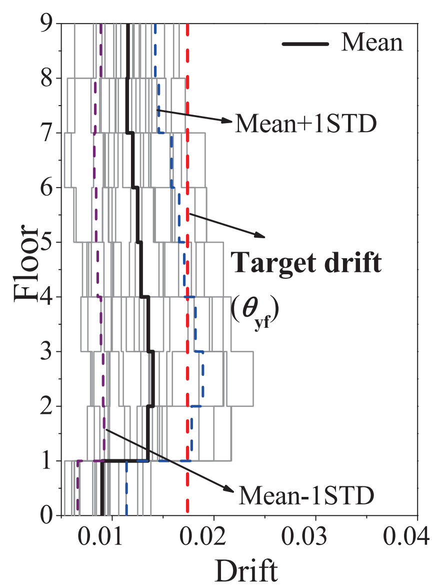

(c)

Fig. 11 Maximum inter-storey drift responses of the designed hybrid steel MRF with EDBs: (a) 3-storey structure, (b) 6-storey structure and (c) 9-storey structure.

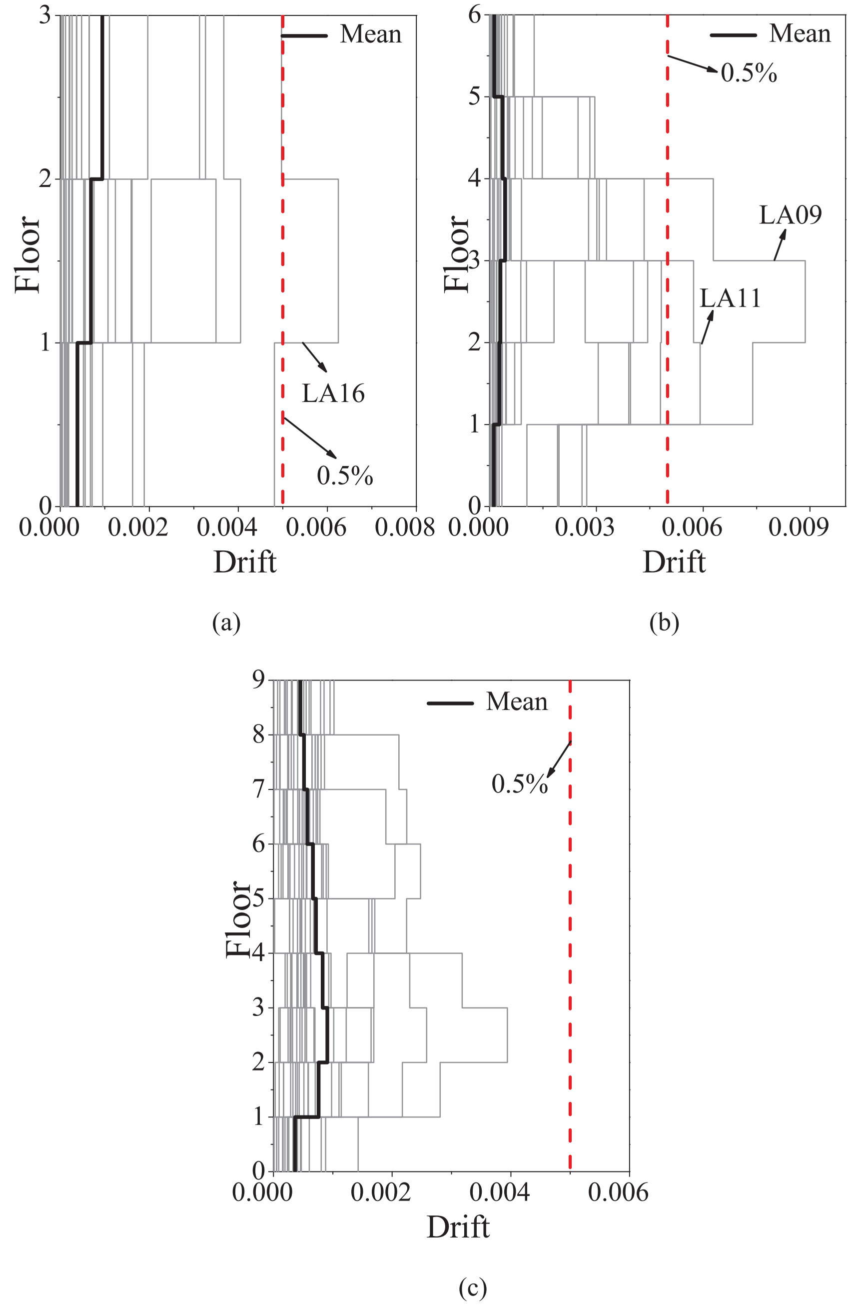

Fig. 12 Residual inter-storey drift responses of the designed hybrid steel MRF with EDBs: (a) 3-storey structure, (b) 6-storey structure and (c) 9-storey structure.

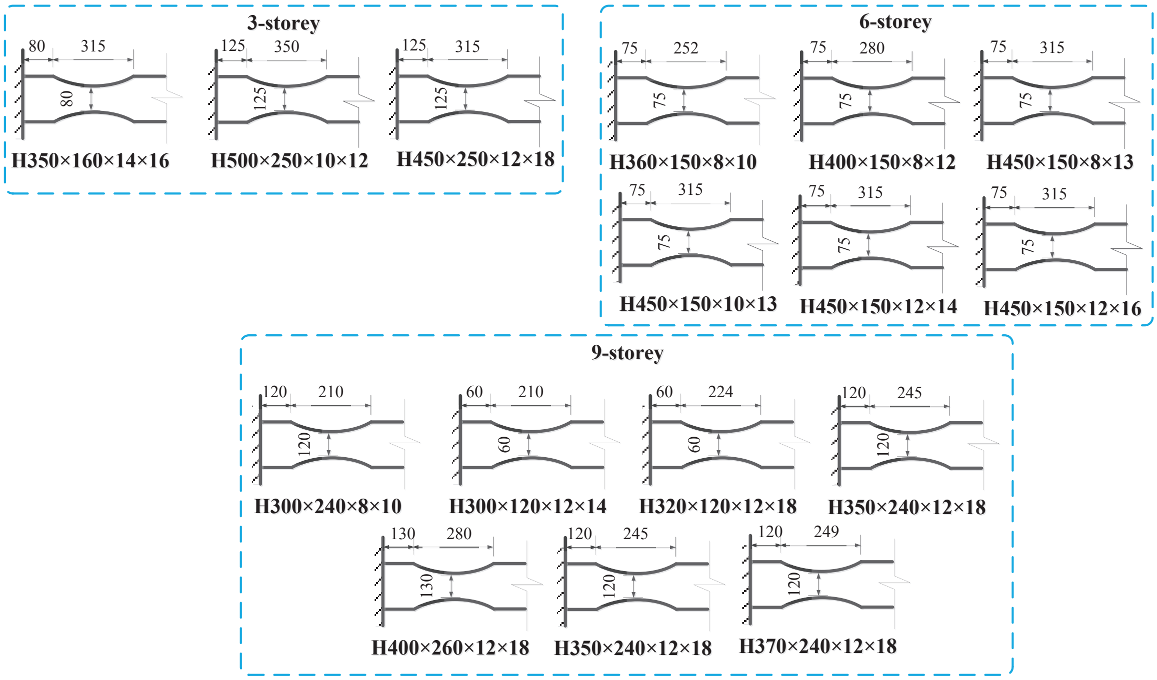

Fig. B.1 Details of RBS in the prototype structures.

Table 1 Specimen detail [8]: member information and material properties

Member	Section	Material property		Column slenderness ratio
		Yield strength f_y (MPa)	Ultimate strength f_u (MPa)	
HSS column	H120×120×12×16	587	642	36~53
HSS beam	H140×100×12×12	504	575	-
Beam in the EDB	H205×75×4×4	338	459	-

Table 2 Design parameters of the prototype structures

Parameters	3-storey	6-storey	9-storey	Notes
Post-yielding stiffness of the damage-control stage, α	0.5 (0.37)	0.6 (0.72)	0.5 (0.50)	Equation (22) satisfied
Yield drift ratio of the main frame to the EDBs, ζ	4 (3.94)	4.5 (6.06)	4 (6.69)	
Energy factor, γ_e	(0.74)	(0.79)	(0.78)	By spectral analyses in the iterative step
Yield drift of EDBs, θ_{ye} (%)	0.4 (0.41)	0.4 (0.33)	0.4 (0.26)	Utilising beams with RBS section
Target drift, $\zeta\theta_{ye}$ (%)	1.6 (1.61)	1.8 (2.01)	1.6 (1.74)	Threshold of the damage-control stage
Fundamental period, T (s)	0.71	1.55	1.71	Determined by frequency analysis
Spectral acceleration, S_a	0.97	0.48	0.40	Determined from the mean spectrum of ground motions based on T
Seismic weight (kN)	2509	5292	8771	determined according to [43]

Notes: The values in the brackets are determined by step 8 after one iteration.

Table C.1 Storey capacity factor and regularity index of the 3-storey hybrid steel MRF with EDBs

Floor	$^*i_{ns}$	$^*i_{os}$	$^*i_{sc}$	$^*\alpha_{sc}$
1	0.83	1	0.99	0.94
2	1	0.76	0.90	
3	0.86	0.98	1.00	

Table C.2 Storey capacity factor and regularity index of the 6-storey hybrid steel MRF with EDBs

Floor	$*i_{ns}$	$*i_{os}$	$*i_{sc}$	$*\alpha_{sc}$
1	0.62	1.00	0.84	0.90
2	1.00	0.71	0.97	
3	0.95	0.74	0.96	
4	0.90	0.78	0.96	
5	0.81	0.91	1.00	
6	0.61	1.00	0.83	

Table C.3 Storey capacity factor and regularity index of the 9-storey hybrid steel MRF with EDBs

Floor	$*i_{ns}$	$*i_{os}$	$*i_{sc}$	$*\alpha_{sc}$
1	0.65	1.00	1.00	0.97
2	0.98	0.66	0.99	
3	0.96	0.66	0.97	
4	0.94	0.68	0.99	
5	0.90	0.70	0.97	
6	1.01	0.64	1.00	
7	1.00	0.65	1.00	
8	0.97	0.68	1.01	
9	0.65	1.00	1.00	

*Notes: i_{ns} is the stiffness factor given in Equation (A.2); i_{os} is the strength factor, given in Equation (A.3); i_{sc} is the storey capacity factor given in Equation (A.1) and α_{sc} is the regularity index given in Equation (24).